IET Microwaves, Antennas & Propagation

Research Article

Optimisation and implementation for a non-focal Rotman lens design

ISSN 1751-8725
Received on 25th November 2014
Revised on 29th January 2015
Accepted on 30th January 2015
doi: 10.1049/iet-map.2014.0797
www.ietdl.org

Mojtaba Rajabalian[1], *Bijan Zakeri*[2] ✉

[1]*Department of Electrical and Computer Engineering, Babol Noshirvani University of Technology, Babol, Iran*
[2]*Faculty of Electrical and Computer Engineering, Babol Noshirvani University of Technology, Babol, Iran*
✉ *E-mail: zakeri@nit.ac.ir*

Abstract: Rotman lens is widely used to feed a phased array antenna to implement a beam forming network. In designing Rotman lens, one of the most important challenges is the phase error. In recent years, Rotman lens has been designed by using a non-focal idea whereas the position of ports are only optimised to reduce the phase error. Because of the unsuitable location of the ports, which causes mismatching and coupling, the previous non-focal method cannot be constructed easily. To implement the lens, a new scheme, converting three-focal Rotman lens to non-focal, is presented. By using a simple procedure, the phase error is properly reduced. To evaluate the proposed method, the non-focal Rotman lens has been implemented at 10 GHz. The simulation and measurement results illustrate that the method is implementable. Furthermore, the average improvement of the maximum phase error in the proposed lens, with five beam ports and five array ports with overall lens size of 15×15 cm^2, is 36% better than the previous reported work.

1 Introduction

For decades, Rotman lens has been used as beam forming network (BFN) because of its individual features such as bandwidth, true time delay, easy implementation, inexpensiveness and compactness [1, 2]. By using the microstrip technology, its applications, such as radar [3], remote sensing, collision avoidance [4], optic searcher [5], reconfigurable beam former, point-to-point communication, satellite communication and direction finding [6], have been developed rapidly. In 2008, a new plan to reduce its insertion loss has been proposed [7]. Furthermore, its gain and compactness can be simultaneously realised by using the substrate-integrated waveguide (SIW) [8, 9] and silicon wafer [10, 11] technologies. Moreover, it has been implemented as microwave switch, multiplexer [12, 13] and multi-layer configuration beam steering [14, 15].

The challenge in these investigations is the phase error. When the number of output ports increases, the phase error will also arose. Researchers have proposed several methods to reduce the phase error [16–20]. In the published work by Dong [19] at 2010, a non-focal method for designing and optimising the phase error has been reported. However, the position of the ports is only optimised to reduce the phase error. It was not appropriate for implementation because of their port positions. In this paper in order to reduce the phase error, a method converting three-focal to non-focal is presented. The problem introduced by Dong is overcame by using the proposed method.

In the first section, the structure of Rotman lens and its performance have been introduced. In the next section, after introducing the design methods, the proposed method has been described. To evaluate the method, a non-focal lens with five input and five output ports has been designed, implemented and tested at 10 GHz. For further evaluation, another lens has been designed at 16 GHz and only simulated to demonstrate the advantage of the proposed method. Final results are presented in the last section.

2 Background

Rotman lens consists of two parallel metal plates that guide and force the wave to transmit various paths that produces different phase shifts [1]. Generally, this lens has a number of input and output ports. Output ports are connected to the phase array antenna using limited transmission lines. The excitation of the each port produces different phases for radiating elements to align the beam in desired direction.

In recent years, three methods have been developed to design a Rotman lens. These methods are three-focal, quadru-focal and non-focal. In designing Rotman lens with three focal ports, three ideal ports are chosen to obtain zero error. However, in other ports, the phase error occurs. Many methods are introduced to reduce the error [16–18]. Rotman lens by using four focal ports has zero phase error that is ideal to 3D phased array radars. This kind of design is not used because of its error and hardship. By using an evolutionary optimisation algorithm, a non-focal Rotman lens can be produced. All of input and output ports are designed to reduce the maximum or mean value of the phase error. Hence, the maximum phase error in non-focal design is reduced in comparison with other methods. However, in non-focal Rotman lens there are more complexities which will be solved in Section 2.4.

2.1 Conventional method

Fig. 1 illustrates the general structure of a conventional three-focal Rotman lens. Its parameters are presented in Table 1.

Based on Fig. 1, there are two curves; input and output ports curves located in the left and right of the structure, respectively. Input ports are specified by (X, Y) from the origin. Positions, specified by N, are array elements. Three focal ports G1, F2 and F1 can be seen in the figure. By exciting these ports, the direction of radiation will be $-\alpha$, $+\alpha$ and 0°. Phase errors of these focal ports are zero. By determining α, φ, ε_r and ε_{eff}, which depend on our design, x, y and w can be found as [2]

$$y = \frac{b_1}{b_0} n \left(\frac{1}{\sqrt{\varepsilon_r}} - \frac{\sqrt{\varepsilon_{eff}}}{\varepsilon_r} w \right) \tag{1}$$

$$x^2 + y^2 + 2gx = \frac{\varepsilon_{eff}}{\varepsilon_r} w^2 - 2 \frac{\sqrt{\varepsilon_{eff}}}{\sqrt{\varepsilon_r}} gw \tag{2}$$

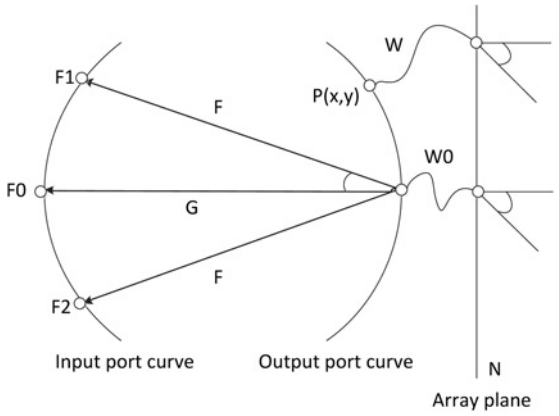

Fig. 1 *Rotman lens including input and output ports curves as well as lines and array elements*

Table 1 Parameters of three-focal Rotman lens

Description	Parameters
central focal port	$G1$
upper focal port	$F1$
lower focal port	$F2$
focal ports angle	α
radiation angle of the array elements	φ
central focal port/side focal port	G/F
input ports coordinate	(X, Y)
array elements position	N
relative permittivity	ε_r
effective permittivity	ε_{eff}
length of the output transmission line	w

$$aw^2 + bw + c = 0 \tag{3}$$

where

$$a = \frac{\varepsilon_{eff}}{\varepsilon_r} - n^2\left(\frac{b_1}{b_0}\right)^2\frac{\varepsilon_{eff}}{\varepsilon_r^2} - \frac{\varepsilon_{eff}}{\varepsilon_r}\frac{(g-1)^2}{(g-a_0)^2} \tag{4}$$

$$b = 2\sqrt{\frac{\varepsilon_{eff}}{\varepsilon_r}}\frac{g(g-1)}{(g-a_0)} - \frac{1}{\varepsilon_r}\sqrt{\frac{\varepsilon_{eff}}{\varepsilon_r}}\frac{(g-1)b_1^2n^2}{(g-a_0)^2} + \frac{2}{\varepsilon_r}\sqrt{\frac{\varepsilon_{eff}}{\varepsilon_r}}\left(\frac{b_1}{b_0}\right)^2 - 2\sqrt{\frac{\varepsilon_{eff}}{\varepsilon_r}}g \tag{5}$$

$$c = \frac{(b_1n)^2g}{\varepsilon_r(g-a_0)} - \frac{(b_1n)^4}{4\varepsilon_r^2(g-a_0)^2} - \left(\frac{b_1}{b_0}\right)^2\frac{n^2}{\varepsilon_r} \tag{6}$$

with $a_0 = \cos\alpha$, $b_0 = \sin\alpha$, $a_1 = \cos\varphi$ and $b_1 = \sin\varphi$.

2.2 Phase error calculation as objective function

Each excitation produces a particular wave front in the space. This phase depends on the beam production angle. If the occurred phase has more deviations from the considered phase, a large phase error will be formed. Each point on the wave front has an identical phase. By exciting each port, the path traversed by the wave should be identical to the wave front, resulting in the maximum field in designed direction. Consequently, as can be seen in Fig. 2, the beam will be positioned parallel to φ_s indicating the wave front direction. Therefore the phase error in

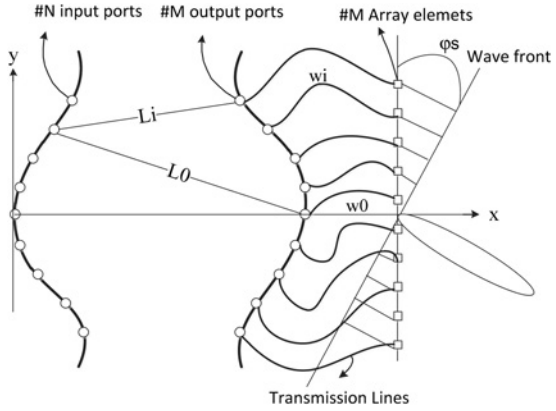

Fig. 2 *Wave front and phase error of the lens*

degree is calculated by

$$\frac{360}{\lambda}[(L_i\sqrt{\varepsilon_r} + W_i\sqrt{\varepsilon_{eff}} + y\sin\varphi_s) - (L_0\sqrt{\varepsilon_r} + W_0\sqrt{\varepsilon_{eff}})] \tag{7}$$

Rotman utilised this design based on three equations in focal ports. Therefore the phase error will be zero in the focal ports. However, a noticeable phase error is found in the non-focal ports. When non-focal ports are far from the focal, their phase errors will be increased rapidly. Hence, in large apertures, the phase error is considerable and the performance of the lens decreases.

2.3 Non-focal Rotman lens

In these investigations, the aim is to minimise the phase error in all ports. Initially, the number of input ports and desired angles are specified. In the next step, G/D parameter, where D defines length of array elements, is specified. The phase error optimisation and their comparison should be based on the constant of G/D. Owing to (7), which illustrates the phase error, primary quantities for the position of the ports and the length of transmission lines are considered. By using an evolutionary algorithm, these positions are calculated to reach the minimum possible phase error [19]. The cycle will be repeated while the expected phase error or the number of update cycles approaches to the defined value.

The phase error reduction, proposed in this work, is better than three focal designs introduced in the literatures. As previously mentioned, the locations and lengths can be optimised by well-known methods such as genetic algorithm and particle swarm optimisation (PSO). The position of the ports may be close or far from each other. They disturb the phase in the excitation time. Consequently, any implementable plan has not been proposed in the previous works. In the following section, we present an implementable method that improves the phase error.

2.4 Procedure to design an implementable non-focal Rotman lens

As mentioned, non-focal lens presented by Dong [19] decreases the phase error without proposing any plan to construct. In our proposed method, by using a recursive scheme, the new positions of the ports are organised. The proposed method is a mixture of three-focal and non-focal method. It has lower error than three focal and is implementable in comparison to previous non-focal method. Unlike Dong's method, the input and output ports are not directly involved in the optimisation process.

According to Fig. 3, in the first step, the positions of the ports are exactly obtained from (1) and (2). In the second step, by using PSO, the length of the transmission lines, to achieve the minimum possible phase error, will be optimised. In the third step, lengths will be substituted in (1) and (2) to update positions of the ports. In the

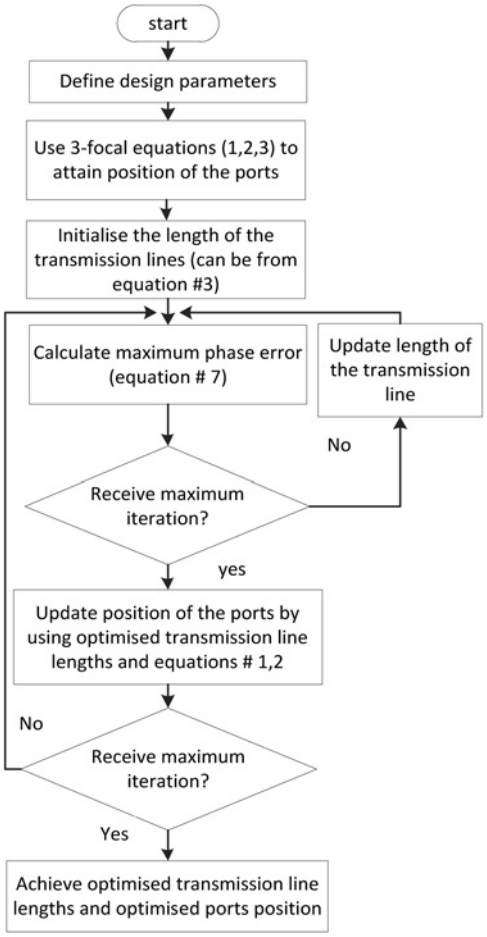

Fig. 3 *Optimisation flowchart of the proposed method*

last step, the procedure should be continued to minimise the phase error. Consequently, the new position of the ports has appropriate distance to implement the lens.

3 Simulation and measurement

To evaluate the proposed method, one lens with five input and five output ports has been designed, implemented and tested at 10 GHz. For further evaluation, another lens has been only simulated at 16 GHz. The design parameters are chosen to minimise the phase error in three-focal method, as listed in Table 2. After optimising, the phase improvement of non-focal method has been compared with three-focal lens.

Table 3 shows primary parameters of PSO algorithm. Since the objective function (7) is simple, there is no special sensitivity for

Table 2 Specification of the proposed lenses

Sign	Description	Lens #1	Lens #2
f_0	design frequency	10 GHz	16 GHz
φ_m	maximum search angle	20°	16°
A	alpha ratio	1	0.8
N	number of input ports	5	7
M	number of output ports	5	16
ε_r	relative permittivity	2.2	2.33
tan δ	loss tangent	0.0012	0.0005
d	element spacing	$\lambda_0/2$	$\lambda_0/2$
h	dielectric thickness	0.25 mm	0.508 mm
t	conductor thickness	0.018 mm	0.018 mm
w	transmission line widths	1.526 mm	0.7814 mm

Table 3 Value of the PSO algorithm parameters

Value	PSO algorithm parameters
30	particle numbers
[0–wavelength]	particle limits
1000	number of iterations
0.3	W min
0.8	W max
2	$C1$
2	$C2$

tuning the parameters. As can be seen in Fig. 4, the ports have appropriate distances from each other. Moreover, optimised transmission lines can be seen in these configurations.

Fig. 5 illustrates the maximum phase errors of three-focal and non-focal designs. Moreover, Table 4 describes the maximum phase error improvement. This table precisely shows improvement in the performance. As can be seen, the optimisation of the side ports is more effective than middle ones. The optimisation will be more effective for larger apertures unlike three-focal method.

Consequently, the proposed method will be effective for all ports except focal port. In the focal ports, the phase error is zero whereas in the other ports the error will be increased. In the presented method, the aim is to minimise the average phase error for all ports, whereas in the three-focal method, the error is small for focal ports only. Furthermore in the three-focal lens, if the number of ports increases, the phase error for the other ports will arose. In the first lens, that is, 10 GHz, there is 181% improvement in the maximum phase error and 36.2% in the average. Moreover, in the second lens the maximum and average improvement of the phase errors are 256.78 and 36.68%, respectively.

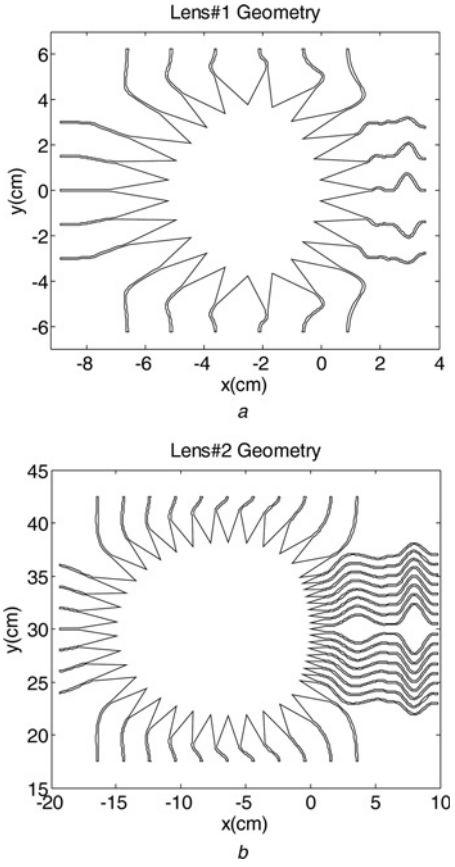

Fig. 4 *Proposed lenses*

a Lens #1 at 10 GHz
b Lens #2 at 16 GHz

IET Microw. Antennas Propag., 2015, Vol. 9, Iss. 9, pp. 982–987

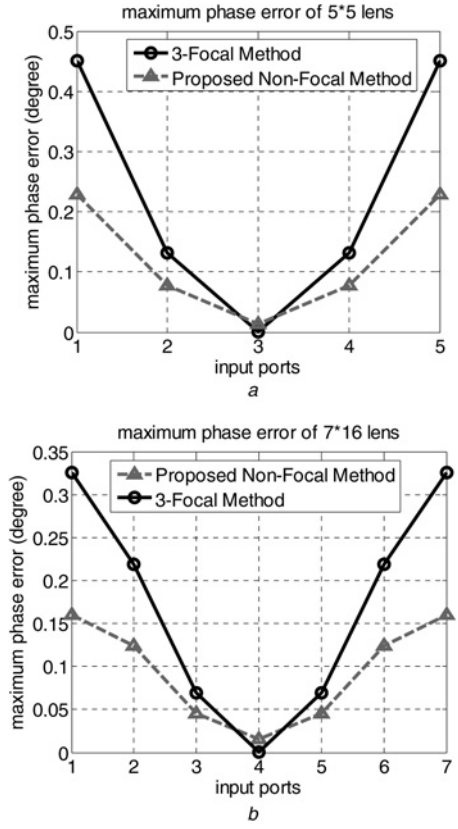

Fig. 5 *Maximum phase error*

a Lens #1
b Lens #2

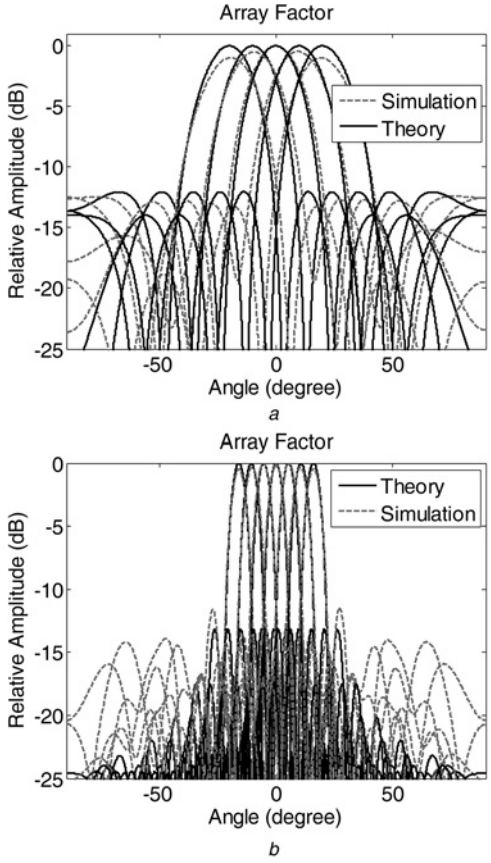

Fig. 6 *Theory and full-wave simulation array factor of lenses*

a Lens #1
b Lens #2

3.1 Full-wave simulation

Full-wave simulation of Rotman lens can predict its performance with a good approximation [21–23]. Fig. 6 illustrates the array factor of designed lens using the new method in theory and full wave simulation. According to the figure, it is evident that the angle of the produced beam matches with theory excellently and verifies the role of the proposed method. The amplitude of the array factor is different with theory because of the coupling, inner reflections and impedance mismatching.

3.2 Measurement results

Fig. 7 shows the implemented lens and its parameters are listed in Table 1. The proposed lens produces beam angles which are directed between −20° and +20° in five steps. If the phase error is small, the produced beam angle will be agreed to theory.

Tables 5 and 6 show the produced beam angle in different methods. As can be understood, the produced beam angle is

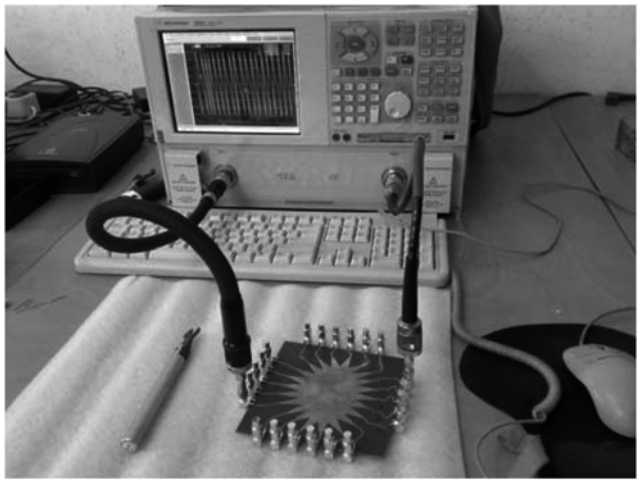

Fig. 7 *Measurement of the proposed lens in 10 GHz*

Table 4 Maximum improvement of phase error for designed lens #1 and lens #2

Lens #1		Lens #2	
Input port number	Maximum phase error, %	Input port number	Maximum phase error, %
1	50.80	1	49.47
2	43.58	2	41.03
3	34.01	3	0
4	0	4	41.03
5	34.01	5	49.47
6	43.58	—	—
7	50.80	—	—

Table 5 Angle of the produced beam in different conditions for lens #2

Port number	Ideal beam angle	Three-focal beam angle (theory)	Proposed method beam angle (theory)	Proposed method beam angle (full-wave simulation)
1	−16	−15.46	−15.95	−15.94
2	−10.66	−10.365	−10.63	−10.36
3	−5.33	−5.151	−5.31	−5.31
4	0	0.0017	−0.113	0.090
5	5.33	5.151	5.31	5.49
6	10.66	10.365	10.63	10.36
7	16	15.46	15.95	15.94

Table 6 Angle of the produced beam in different conditions for lens #1

Port number	Ideal beam angle	Three-focal beam angle (theory)	Proposed method beam angle (theory)	Proposed method beam angle (full-wave simulation)	Proposed method beam angle (measurement)
1	20	19.271	19.89	19.847	19.8290
2	10	9.64	9.91	9.8920	9.8740
3	0	0.099	0.187	0.1710	0.1530
4	−10	−9.64	−9.91	−9.8920	−9.8740
5	−20	−19.271	−19.89	−19.847	−19.8290

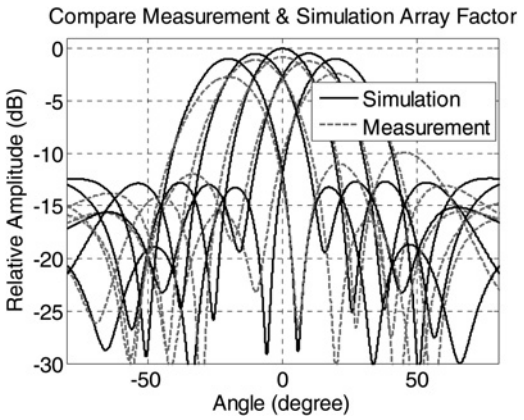

Fig. 8 *Full-wave simulation and measurement array factors for the proposed lens calculated from S-parameters data at 10 GHz*

improved in all ports except in the middle. The beam angle in the first and second lens gets closer to 1.73° and 1.6°, respectively, presenting an ideal situation. The full-wave simulation agrees with the theory very well and verifies the proposed method.

Fig. 8 and Table 6 compare the simulated array factor with the measurement results. As can be seen, the beam production angles are very close to an ideal condition, and the measurement results are very close to the simulation. However, according to sidelobe level, the simulation array factor is better than measurement. Fig. 9 compares the simulated return loss with the measurement results for input ports #1 to #3. Because of the symmetry, return loss of the ports #4 and #5 are equal to ports #2 and #1, respectively. Fig. 10 compares the simulated insertion loss with the measurement results for input ports #1 and #3 only. As can be seen, the measurement shows a significant loss generated by connectors.

4 Discussion and conclusion

The method presented in this paper converts a three-focal Rotman lens to a non-focal to reduce the phase error. In three-focal method with increasing ports, the phase error increases. This problem is one of the most important disadvantages of three-focal. By the presented optimisation, we can eliminate this challenge precisely. Hence, we can design Rotman lens with many ports and small phase errors. In addition, this method has a simple procedure, to implement, with respect to the non-focal method introduced by J. Dong. Input and output ports are updated after optimising the length of transmission lines by three-focal scenario. This makes us to have the ports including appropriate distances from each other to fabricate. The phase error is improved with respect to the three-focal design. Furthermore, for a wider aperture, the improvement for side ports increases with respect to three-focal, as can be seen in Tables 4–6 and Fig. 5. It means that the presented method will be more effective than three-focal.

To evaluate the proposed method, lens #1 including five input/output ports has been designed, implemented and measured at 10 GHz. Furthermore, lens #2 has been designed and full-wave simulated at 16 GHz to more assessments without fabrication. Simulation and measured results show that the first lens has 181

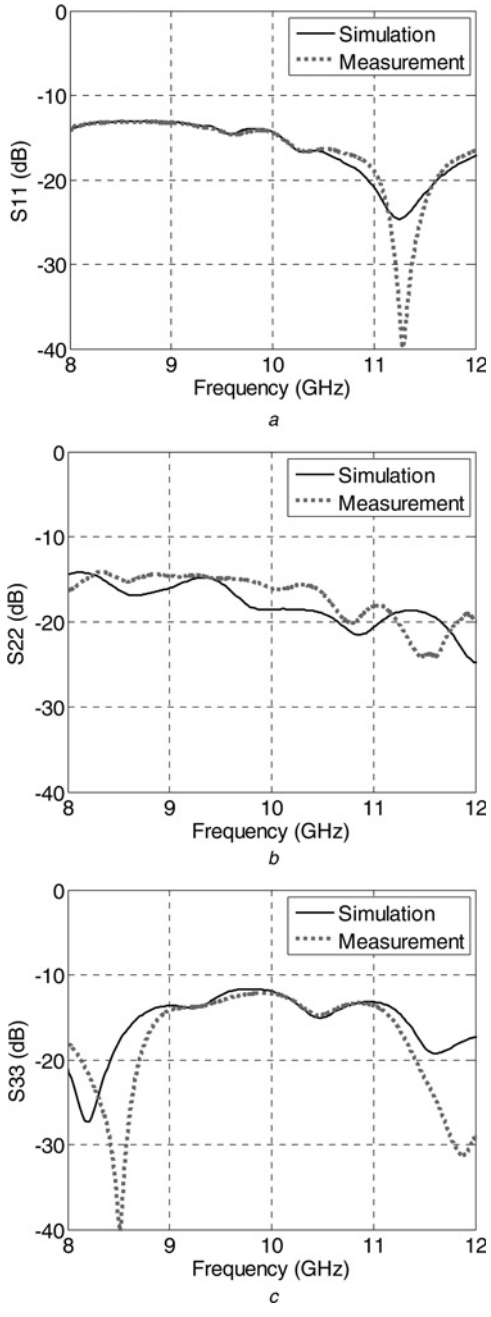

Fig. 9 *Measured and simulated return loss of the proposed lens*
a S_{11}
b S_{22}
c S_{33}

and 36.2% improvement in the maximum and mean phase errors, respectively. Furthermore, for lens #2, the previous parameters are 256.78 and 36.68%, respectively. The beam production angles in the first and second lens are 1.61° and 1.73° closer to the ideal state. These results illustrate that the presented method can be

IET Microw. Antennas Propag., 2015, Vol. 9, Iss. 9, pp. 982–987

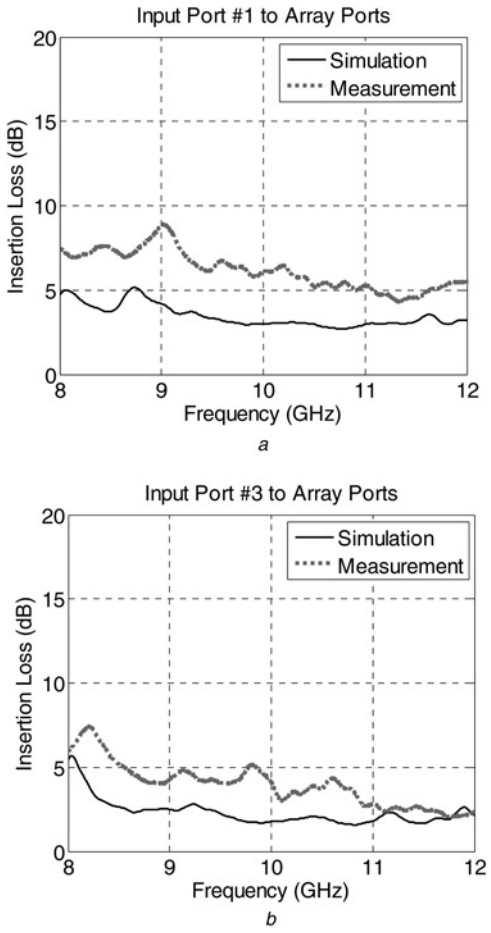

Fig. 10 *Measured and simulated insertion loss of the proposed lens for ports #1 and #3*

implemented and constructed appropriately and it is able to improve average of maximum phase error by more than 36% in lens design compared to previous three-focal method.

5 Acknowledgments

The authors would like to thank all the people in microwave centre at Sazgan Ertebat Co. for providing a great experience in training cutting-edge microwave technology. In particular, many private discussions with Sh. Mehdinia and E. Soltani have been immensely helpful in testing.

6 References

1 Rotman, W., Turner, R.: 'Wide-angle microwave lens for line source applications', *IEEE Trans. Antennas Propag.*, 1963, **11**, pp. 623–632
2 Herd, J.S., Pozar, David, M.: 'Design of a microstrip antenna array fed by a Rotman lens'. Antennas and Propagation Society Int. Symp., 1984, vol. 22, pp. 25–29
3 Kilic, O., Dahlstrom, R.: 'Rotman lens beam formers for Army multifunction RF antenna applications'. IEEE Antennas and Propagation Society Int. Symp., 3–8 July 2005, vol. 2B, pp. 43–46
4 Dong, J., Zaghloul, A.I.: 'Extremely high-frequency beam steerable lens-fed antenna for vehicular sensor applications', *IET Microw. Antennas Propag.*, 2010, **4**, (10), pp. 1549–1558
5 Rotman, R., Rotman, S., Rotman, W.: 'Wideband RF beam-forming: the Rotman lens vs. photonic beam-forming'. IEEE Antennas Propagation Society Int. Symp., 2005, vol. 2B, pp. 23–26
6 Zhang, Y., Christie, S., Fusco, V.: 'Reconfigurable beam forming using phase-aligned Rotman lens', *IET Microw. Antennas Propag.*, 2012, **6**, (3), pp. 326–330
7 Schulwitz, L., Mortazawi, A.: 'A new low loss Rotman lens design using a graded dielectric substrate', *IEEE Trans. Microw. Theory Tech.*, 2008, **56**, (12), pp. 2734–2741
8 Cheng, Y.J., Hong, W., Wu, K., Kuai, Z.Q.: 'Substrate integrated waveguide (SIW) Rotman lens and its Ka-band multibeam array antenna applications', *IEEE Trans. Antennas Propag.*, 2008, **56**, (8), pp. 2504–2513
9 Tekkouk, K., Ettorre, M., Sauleau, R.: 'Compact multibeam Rotman lens antenna in SIW technology'. IEEE Antennas and Propagation Society Int. Symp. (APSURSI), July 2012, pp. 1–2, 8–14
10 Lee, W., Kim, J., Cho, C., Yoon, Y.J.: 'Beam forming lens antenna on a high resistivity silicon wafer for 60 GHz WPAN', *IEEE Trans. Antennas Propag.*, 2010, **58**, (3), pp. 706–713
11 Attaran, A., Chowdhury, S.: 'Fabrication of a 77 GHz Rotman lens on a high resistivity silicon wafer using lift-off process', *Int. J. Antennas Propag.*, 2014, 9 pages
12 Zhang, Y., Fusco, V.: 'Rotman lens used as a demultiplexer/multiplexer'. 42nd European Microwave Conf. (EUMC), 2012, pp. 164–167
13 Zhang, Y., Fusco, V.: 'N-way switch based on Rotman lens', *Electron. Lett.*, 2012, **48**, (5), pp. 270–271
14 Kim, J., Lee, W., Yoon, Y.J.: 'Multilayer Rotman lens fed antenna array for system packaging'. Int. Symp. on Antennas and Propagation (ISAP), 2012, pp. 664–667
15 Lambrecht, A., Laskowski, P., Beer, S.: 'Frequency invariant beam steering for short-pulse systems with a Rotman lens', *Int. J. Antennas Propag.*, 2010, 8 pages
16 Katagi, T., Mano, S., Sato, S., Tahara, S.: 'An improved design method of Rotman lens antennas', *IEEE Trans. Antennas Propag.*, 1982, **20**, pp. 136–139
17 Smith, M.S.: 'Design considerations for Ruze and Rotman lens', *The Radio Electron. Engr.*, 1982, **52**, pp. 181–187
18 Hansen, R.C.: 'Design trades for Rotman lenses', *IEEE Trans. Antennas Propag.*, 1991, **39**, pp. 464–472
19 Dong, J., Zaghloul, A.I., Rotman, R.: 'Phase-error performance of multi-focal and non-focal two-dimensional Rotman lens designs', *IET Microw. Antennas Propag.*, 2010, **4**, (12), pp. 2097–2103
20 Rajabalian, M., Zakeri, B.: 'Non-focal microwave lens design with optimization of phase errors and amplitude performance'. Twentieth IEEE Telecommunications Forum (TELFOR 2012), 20–22 November 2012, pp. 1179–1182
21 Penney, C., Luebbers, R.J., Lenzing, E.: 'Broad band Rotman lens simulations in FDTD'. Antennas and Propagation Society Int. Symp., IEEE, 2005, vol. 2B, pp. 51–54
22 Dong, J., Zaghloul, A.I., Rotman, R.: 'A fast ray tracing method for microstrip Rotman lens analysis'. URSI General Assembly Chicago, 2008
23 Nazari, M., Ghorbani, A., Moradi, A.: 'An ultra-wideband Rotman lens using modified dummy sidewalls', *IEICE Electron. Express*, 2001, **8**, (15), pp. 1228–1233